Diffraction-limited Microbeam with Fresnel Zone Plate Optics in Hard X-Ray Regions

Yoshio Suzuki,[*a] Akihisa Takeuchi,[a] Hidekazu Takano,[a] Takuji Ohigashi[b] and Hisataka Takenaka[c]

[a]SPring-8, Mikazuki, Hyogo 679-5198, Japan

[b]Institute of Applied Physics, University of Tsukuba, Tsukuba, Ibaraki 305-8573, Japan

[c]NTT Advanced Technology Corporation, Musashino, Tokyo 180-8585, Japan

ABSTRACT

X-ray microbeam using Fresnel zone plate as a beam focusing device has been tested at an undulator beamline of SPring-8. The zone material is tantalum with thickness of 1 μm, and the zone structure is fabricated by using electron beam lithography technique. The outermost zone width of the zone plate is 0.25 μm. By utilizing a fully coherent illumination, a focused spot size near to the diffraction-limit (0.3 μm) has been achieved at an X-ray energy of 8 keV. The measured beam profiles shows good agreement with the theoretical profile. The measured diffraction efficiency agrees well with theoretical value within an X-ray energy region from 6 keV to 10 keV. A scanning microscopy experiment has also been performed in order to evaluate the spatial resolution. Fine structures of up to 0.2 μm are clearly observed in the measured image. The modulation transfer function derived from the measured image is 10 % at 0.2 μm line and 0.2 μm space.

Keywords: Fresnel zone plate, X-ray microbeam, X-ray microscopy, undulator.

1. INTRODUCTION

Many types of optical systems are developed for generating hard X-ray microbeams.[1-15] Total reflection mirrors, multi-layer mirrors, zone plate optics, refractive lens are tested and applied to microscopy. However, the achieved spatial resolution is still far from theoretical limit. The Fresnel zone plates (FZP) fabricated by electron beam lithography technique are widely used in soft X-ray microscopy, and they achieve the diffraction-limited resolution. The best record of spatial resolution, at present, is better than 30 nm in soft X-ray regions. In the hard X-ray region, it is difficult to use the FZP dedicated to the soft X-ray region, as it is. That is because the zone thickness required for hard X-rays is much larger than that for the soft X-rays. For example, appropriate zone thickness for 10 keV X-rays is estimated to be about 2 μm even for the high density material (gold or tantalum). However, if the zone plate with sufficient thickness can be fabricated, it is expected that the FZP could have the diffraction-limited resolution even in the hard X-ray regions, as is the FZP for soft X-rays. The accuracy of electron beam drawing technique is essentially same as that for the fabrication process for soft X-ray zone plates.
Recently, by using reactive dry-etching process developed for semiconductor devices, aspect ratio higher than 10 is available for tantalum zone plates. It is well known that the spatial resolution of the FZP microscope is determined by the outermost zone width. Therefore, using the high aspect ratio FZP, X-ray microscope with spatial resolution better than that of optical microscopes can be made by using the FZP optics. When the structure of the FZP is sufficiently precise, and the illuminating beam is fully coherent, the focused beam size becomes the diffraction-limited dimension, ie., $1.22d_N$, where d_N is width of outermost zone.

Recently we have tested a newly developed Fresnel zone plate, and the preliminary results have already been reported.[16] In this paper, we describe more details on the evaluation of the X-ray focusing properties. Experiments on scanning microscopy are also done using a resolution test pattern as a test object in order to evaluate the performance of the microprobe. These results are also presented.

---

*Correspondence: E-mail: yoshio@spring8.or.jp; Telephone: +81-791-58-0833; Fax: +81-791-58-0830

X-Ray Micro- and Nano-Focusing: Applications and Techniques II, Ian McNulty, Editor, Proceedings of SPIE Vol. 4499 (2001) © 2001 SPIE · 0277-786X/01/$15.00

2. EXPERIMENTAL SETUP

2.1. Optical element: Fresnel zone plate

The Fresnel zone plate used in the experiment is fabricated using an electron-beam lithography technique at the NTT Advanced Technology[17] The zone structure with an outermost zone width of 0.25 μm is made of 1 μm-thick tantalum. The diffraction limit of the focused beam size defined as $1.22d_N$ is 0.3 μm. The diameter of the FZP is 100 μm, and the focal length is 160 mm at an X-ray energy of 8 keV. A center beam stop (2.4 μm-thick gold) of 50 μm diameter is electroplated on the FZP. Therefore, the diffraction-limit for the spatial resolution determined by the width of the outermost zone and by the ratio of apodization (radius of the center stop disc is a half of the FZP radius) is 0.25 μm for the first-order focus. Schematic drawing of the FZP structure is shown in Fig. 1, and the specification parameter is listed in table I.

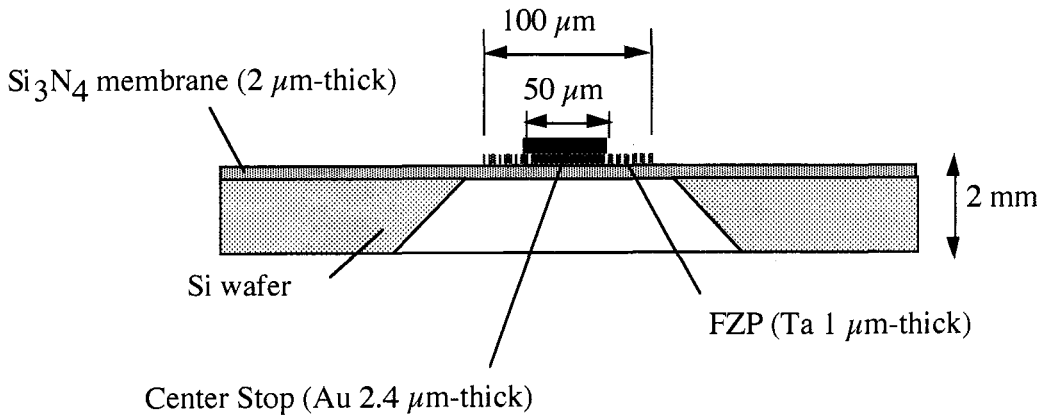

Fig. 1. Schematic drwaing of structure of the Fresnel zone plate

Table I. specification of Fresnel zone plate

Diameter: 100 μm,
Designed focal Length: 160 mm at 8 keV,
Outermost zone width (d_N): 0.25μm,
Diffraction limit (=$1.22d_N$): 0.3 μm,
Numerical aperture: 3.125×10^{-4} at 8 keV,
Zone material: Ta, 1 μm-thick,
Center stop: 50 μm in diameter,
material: Au, 2.4 μm-thick,
Supporting membrane: Si_3N_4, 2 μm-thick.

Fabrication method:
electron-beam lithography technique at NTT-AT

2.2. Optical system

A schematic diagram of the experimental setup is shown in Fig. 2. A planar- type 139 pole undulator[18] installed in SPring-8 8 GeV electron storage ring is used as a light source. The magnetic period of the undulator is 32 mm, and the maximum K-value is 2.3. The stored electron beam current was 100-80 mA during the experiment. The undulator radiation is

monochromatized through a liquid-nitrogen cooled Si 111 SPring-8-standard double-crystal monochromator. Both the first crystal and the second crystal of the monochromator are cooled by liquid-nitrogen, and kept at the same temperature in order to realize a fixed-exit-beam condition.

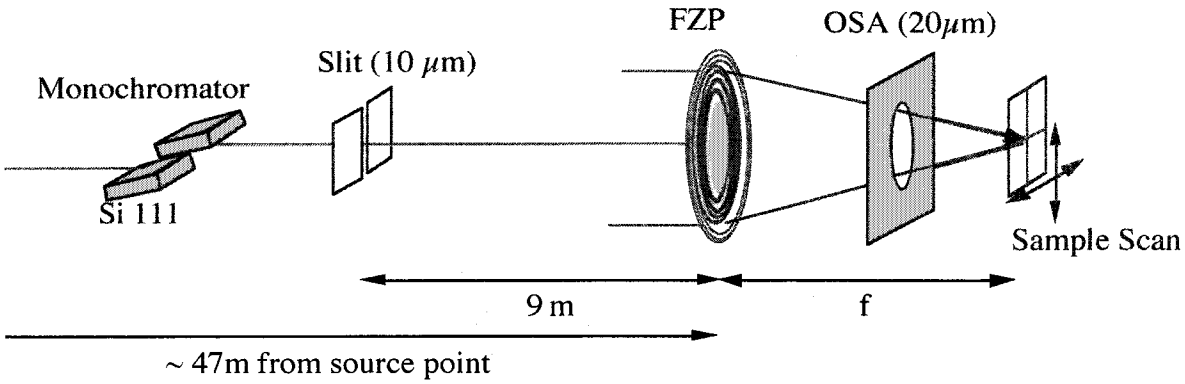

Fig. 2. The experimental setup. OSA: order selecting aperture. FZP: Fresnel zone plate

The monochromatic X-ray beam impinges on a FZP, and is focused at the sample position. The distance between the light source and the experimental station is about 47 m. The vertical source size [about 50 μm in full-width at half-maximum (FWHM)] is fairly small because of a low coupling-constant of the storage ring. Therefore, in the vertical direction, a demagnified image of the undulator light source is produced at the focal point. On the contrary, the horizontal source size (about 0.9 mm in FWHM) is too large to generate a diffraction-limited microbeam. Therefore, a vertical slit with an opening of 10 μm is placed between the monochromator and experimental station. The slit is used as a pseudo-point-like source in the horizontal direction, and the demagnified image of the slit is generated at the focal point. The distance between the slit and the FZP is 9 m. In this optical system, the source location is different between vertical and horizontal foci. Therefore, a kind of astigmatism exists in spite of axial symmetry of the FZP. When the focal length of the optical element is 160 mm, The distance between the FZP and the focusing position is 160.55mm for vertical focus and 162.9mm for the horizontal focus, respectively. Thus the focal points are separated from each other by about 2.4 mm in the longitudinal direction. However, this astigmatism is not very serious for the evaluation of optical elements. The focusing property in each direction can be tested using this configuration.

A pinhole (20 μm in diameter) made in a 0.2-mm-thick Ta plate is placed between the FZP and the focal point in order to select only the first order diffraction. The distance between the FZP and the pinhole is about 130 mm.

The focal spot size is also limited by the geometrical optics, i.e., product of source size and magnification. The magnification (M) is defined by

$$M = f/L,$$

where f (~ 160 mm) is the focal length of the FZP and L (9 m for the horizontal focus, and 47 m for the vertical focus) is the distance between the source point and the FZP. The focal spot size determined by the geometrical optics is 0.17 μm in the vertical direction and 0.18 μm in the horizontal direction for a focal length of 160 mm. They are smaller than the diffraction-limited focused-spot size.

The small astigmatism of the optical system in Fig. 2 can be eliminated by tilting the FZP axis to the optical axis. As shown in Fig. 3, by inclining the FZP by the angle θ, the radius of the n-th Fresnel zone is reduced by a factor of $\cos\theta$, as

$$r_n' = r_n \cos\theta.$$

The focal length, f is expressed by the following formula,

$$r_n^2 = n\lambda f,$$

where λ is X-ray wavelength, and r_n is radius of n-th Fresnel zone. Therefore, the focal length along to the tilting direction is reduced by a factor of $\cos^2\theta$, and the modified focal length f_m can be written as

$$f_m = f \cos^2\theta.$$

The focal length perpendicular to the tilting direction is not varied. The astigmatism can be compensated by using the inclined configuration on FZP optics. There are, of course, some limitation on this inclined geometry. They are aspect ratio of outermost zone structure and the focal depth. The tilting angle θ must be smaller than the aspect ratio as the following formula:

$$\tan\theta < d_N/D,$$

where, d_N is width of outermost zone, and D is the depth of zone structure. For the FZP used in the experiment, d_N = 0.25 μm, and D = 1 μm. Therefore tan θ must be smaller than 0.25. By tilting the FZP, the outermost zone position is shifted along the optical axis by $r_N\sin\theta$. This motion must be smaller than the depth of focus, as follows:

$$2r_N \sin\theta < 0.61\lambda/2/(NA)^2.$$

Where NA is numerical aperture of the FZP. Here, in this experimental setup, the depth of focus is 480 μm at an X-ray energy of 8 keV, and $2r_N$ is 100 μm. Therefore, above conditions are fully satisfied when $\tan\theta$ is smaller than 0.25, i.e., θ < 14 degree. Then, in the present experimental setup, the focal length should be reduced by 1.5% in order to compensate the astigmatism, and the tilting angle becomes 7.1 degree. Consequently, compensation of the astigmatism by the inclined-configuration is valid for the present experimental condition.

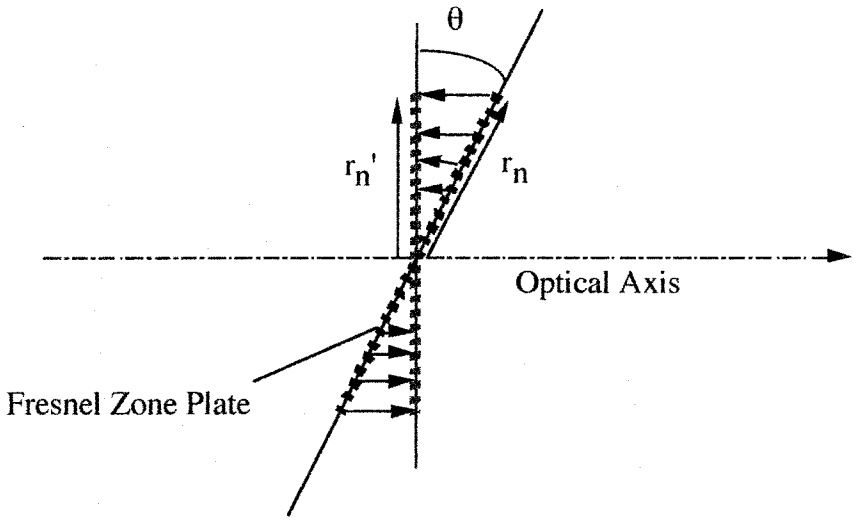

Fig. 3. Inclined geometry for elimination of the astigmatism

2.3. Experimental setup for scanning microscopy

A two-axis translation stage driven by stepping motors is used for sample scanning. The translation stage is commercially available mechanical stages (Kohzu Seiki, type YA-05-14). The stage is translated by a screw of 0.5 mm-pitch. The

stepping motor used for the stages is 5-phase stepping motor (Oriental Motor, PX535MH-B) that is 0.36 degree/step for full-step dirive. By using the micro-step driver [Melec, H-583 (ADB-5410)] for motor control, the minimum step is 1/160 of the full step drive. Therefore, The nominal resolution becomes 1/320 μm/pulse (3.125 nm/pulse). The accuracy of the translating stages is measured with a laser position monitor (Keyence, type LC2420) whose resolution is 0.01 μm. The results are shown in Fig. 3. Although the stage is commercially available mechanical stage, as shown in the figure, accuracy of translation better than 0.01 μm is easily achieved by an open-loop-control system. More precise test can not be done at present, because the LSB of the position monitor is 0.01 μm. However, the results shown in Fig. 3c suggests that the translating stage would have the resolution better than 0.01 μm.

The focal spot size is measured by conventional knife-edge scanning method with this sample scan stage. A gold wire of 50 μm diameter is actually used as the "knife-edge". The intensity of the monochromator output beam is monitored by an ionization chamber (air 1 atm), and the intensity of the focused X-ray beam is also measured with another ionization chamber. The line-spread-function of the focused beam is derived from the numerical differential of the measured knife-edge scan profiles. The scanning X-ray microscopy experiment is also performed by raster-scanning the sample with the two-axis translation stage.

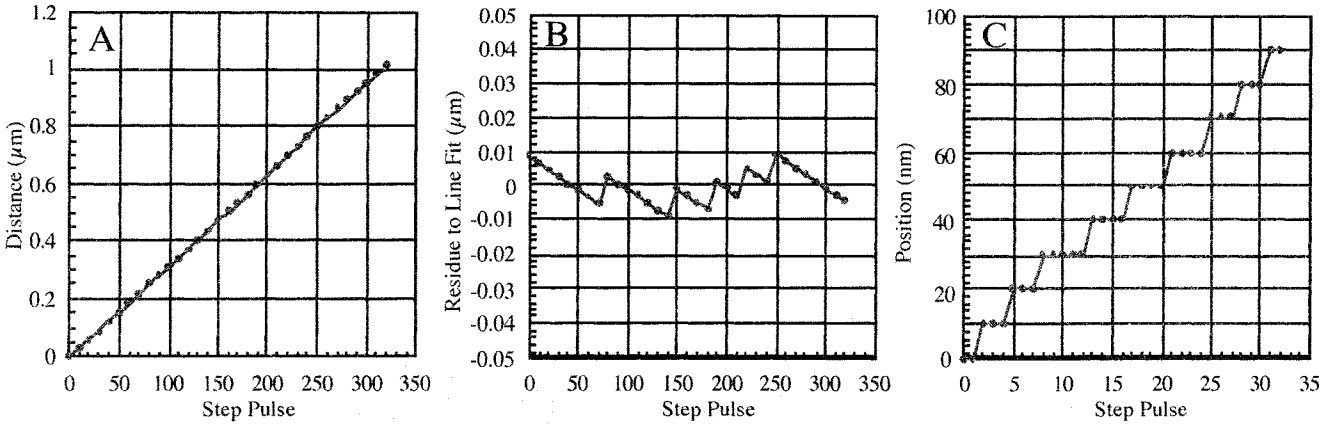

Fig. 4. Measured accuracy of the high-precision translation stage. Fig. A and B is measured data within 1 μm distance. Fig. A represent respnse to step pulse (10 pulse/ step), and Fig. B shows residue to best-fit-line for the data in Fig. A. The response of stage for 1 pusle step is shown in Fig. C.

3. RESULTS

3.1. Focused Beam size

The focused spot size measured by numerical-deferential of the edge-scan profile is shown in Fig. 4. The measured focal spot size in the horizontal direction is 0.3 μm in FWHM. This focal spot size agrees well with the theoretical limit of the FZP with 0.25 μm outermost zone width. The vertical spot size is also measured by the edge-scan method. However, as shown in the figure, the spot size in the vertical direction, 0.5 μm in FWHM, is apparently worse than that in the horizontal direction.

If coherence of the light source is preserved by passing through the beamline, as is mentioned above, the focal spot size in the vertical direction must be equal to that in the horizontal direction. However, there are some factors that may possibly deteriorate the spatial coherence such as roughness of windows, distortion of optical elements and vibration. Three beryllium foils of 0.25 mm thickness are used as vacuum windows of the beamline. However, these Be foils are carefully polished (peak-to-valley roughness of less than 1 μm) in order to avoid distortion of the wave front. The monochromator crystals are thick (35 mm) single crystals, and an indirect liquid nitrogen cooling system is employed, so that the deformation due to heat load or stress is considered to be negligibly small. The most likely cause is vibration of the monochromator crystals.

The vibration of the crystal is checked by measuring the time-structure of the monochromator output beam intensity and the rocking curve profile of the double crystal monochromator. The beam intensity was oscillating with a frequency of 200 Hz. Assuming that the instability of the beam intensity is caused by detuning of the (+, -) double crystal configuration, the

relative angular displacement of the monochromator crystals is estimated to be about 1 μrad from the amplitude of the variation of the beam intensity and the measured rocking curve profile. This vibration is considered to be caused by flow of the coolant. Therefore, it can be considered that the monochromator output beam is vibrated by a factor of 2 μrad. When the angular displacement is $\Delta\theta$, and the focal length is f, the focal spot size is broadened by $\Delta\theta \cdot f$. In the experimental condition, f = 160 mm and $\Delta\theta$ = 2 μrad, the broadening of the spot size becomes 0.32 μm. The measured focus spot size in the vertical direction (0.5 μm) can be explained by taking the broadening into account. We consider that this broadening due to the vibration of monochromator crystals may be the main reason behind the discrepancy between the measured vertical focus spot size and the diffraction limited focus. On the contrary, the horizontal focus spot size is determined by the slit placed downstream from the monochromator. Therefore, the horizontal spot size is not affected by the vibration of the monochromator crystals.

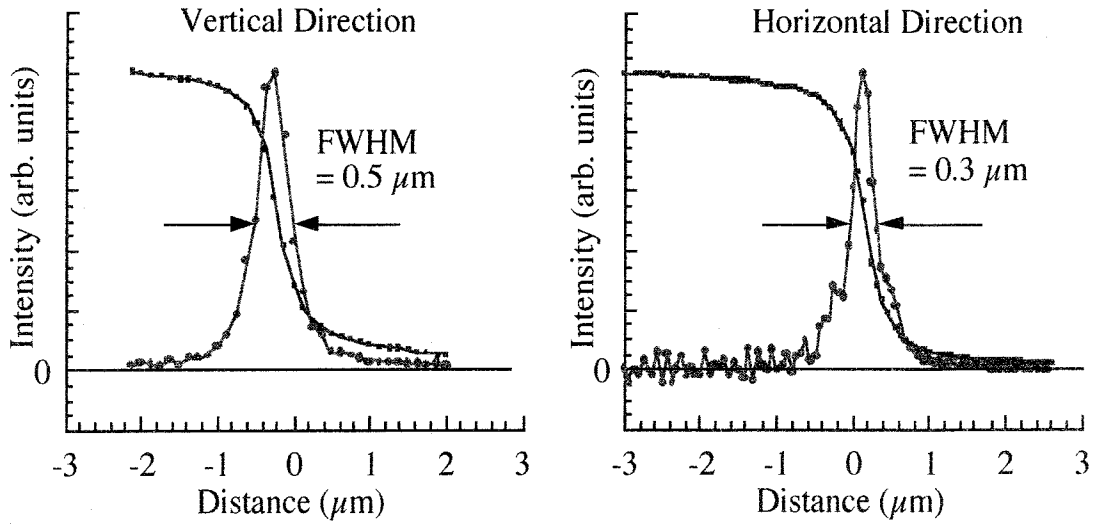

Fig. 5. Focused beam profiles measured by knife-edge scannin: raw intensity data from edge-scan, and the numerical derivative. X-ray energy is 8 keV. The vertical focusing is done by demagnification of the light source image. The horizontal focus is generated by demagnification of a slit image. The vertical slit with width of 10 μm at 9 m upstream of the FZP is used as a pseudo-point-like source.

More detailed analysis for the focusing profile in the horizontal direction has been done. The intensity distribution around the focus, I(r), is described by a wellknown diffraction theory of light.[19] Using the Bessel function, J_1,

$$I(r) = [2J_1(kNAr)/kNAr]^2,$$

where $k=2\pi/\lambda$, NA is numerical aperture of the objective (FZP), and r represents the distance around the optical axis as

$$r = (x^2 + y^2)^{1/2}.$$

When the beam stop with radius of εa (a: radius of FZP) is placed at the center of FZP, the intensity profile is modified as

$$I(r) = 1/(1 - \varepsilon^2)^2 \, [\{2J_1(kNAr)/kNAr\} - \varepsilon^2\{2J_1(k\varepsilon NAr)/k\varepsilon NAr\}]^2.$$

Generally, it is very difficult to measure the point spread function, I(r), directly. The beam profile derived from the knife-edge scan corresponds to the line-spread-function, I(x), that is derived by integral of I(r), as

$$I(x) = \int I((x^2 + y^2)^{1/2})\, dy.$$

When the source has finite dimension, the focused beam profile is also limited by the geometrical optics. Therefore, the focused beam profile,$I_m(x)$, is described by a convolution integral using the focused image profile determined by the geometrical optics, P(X), as

$$I_m(x) = \int I(x + X)\, P(X)\, dX.$$

Using above formula, the theoretical beam profiles, I(x) and $I_m(x)$, is calculated for the present experimental condition. The results are shown in Fig. 4. When the radius of the center stop is a half of FZP radius ($\varepsilon = 0.5$), focused beam size defined by the FWHM is almost equal to the outermost zone width. As shown in Fig. 4, the FWHM of line spread function is 0.237μm for the FZP with 0.25 μm outermost zone width. It is also important that broadening due to the source size is negligibly small, when the geometrical beam size is smaller than the diffraction-limited spot size. The measured beam profile in horizontal direction shows good agreement with the theoretical beam profile. It should be noticed that the secondary maximum is also observed as sholders at 0.35 μm around the main peak. These results indicate that the FZP has good accuracy for application to coherent optics.

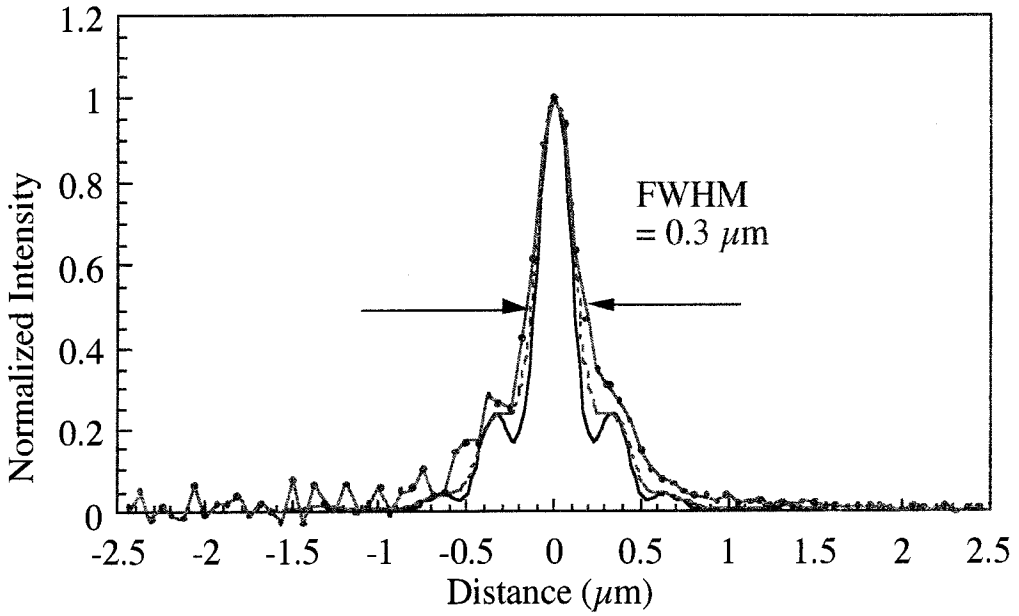

Fig. 6. Calculated beam profile and comparison to measured data. Solid line represents theoretical profile for coherent illumination, and the dashed line represents calculated beam profile by taking the geometrical spot size of 0.18 μm in to account. Closed circles are measured data.

3.2. Diffraction efficiency

The diffraction efficiency is measured by comparing the flux density of X-rays incident on the FZP with the intensity of the focused beam. The measured efficiency for the first-order diffraction is shown in Fig. 6. Theoretical efficiency is also shown in the figure. The theoretical values are calculated by the following formula:

$$\text{Efficiency} = 1/\pi^2(1 + \gamma^2 - 2\gamma \cos(kt\delta)),$$

where

$$\gamma = \exp(-kt\beta),$$

$k = 2\pi/\lambda$,

t: thickness of zone,

$1 - \delta + i\beta = n$: complex index for refraction of zone material.[20]

As shown in the figure, the measured efficiency shows good agreement with theoretical calculation. Diffraction efficiency of about 20% is achieved at 8 keV. The total flux of the microbeam is about 10^9 photons/s for 100 mA stored current at an X-ray energy of 8 keV.
More important feature of the diffraction efficiency is that the second order diffraction was not detectable. Therefore, the FZP is considered to have precise zones within a 0.1 μm-level lateral structure.

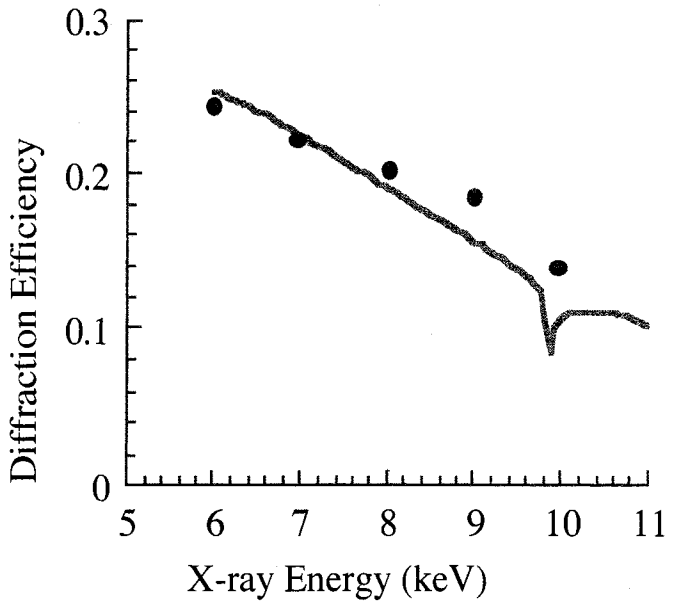

Fig. 7. Efficiency of the first order diffraction. The solid circles are measured data, and the solid line is theoretical calculation.

3.3. Scanning microscopy

The scanning microscopy experiment has been performed for evaluating the performance of the microprobe. Resolution test patterns that is fabricated using the electron-beam lithography technique is used as a test sample. The sample has fine pattern made of 0.5 μm-thick tantalum deposited on Si_3N_4 thin membrane, and its finest structure is a 0.1 μm line-and-space patterns. Results of the scanning microscopy experiment and a schematic drawing of the resolution test patterns are shown in Fig. 4. The transmittance of the 0.5-μm-thick tantalum film is 87% for 8 keV X-rays. Therefore, the contrast of the test pattern is insufficient in the hard X-ray regions. However, as shown in the figure, the fine patterns of up to 0.2-μm-width have been clearly resolved in the measured image.
For the quantitative analysis of the spatial resolution, square-wave modulation-transfer-function (MTF) is extracted from measured image. Results are shown in Fig. 8. Theoretical MTF derived from the line spread function, $I_m(x)$, and the MTF derived from the knife-edge-scan profile are also shown in the figure. The MTF derived from the test-pattern-image and the MTF from the knife-edge-scan agrees well each other. The amplitude response at a spatial frequency of 2.5 μm^{-1} (0.2 μm line and 0.2 μm space) is 10%. The measured MTF fairly agrees with the theoretical value except for reduction of amplitude response by about 10%. The discrepancy is considered to be due to zero-th order light through the center stop. Theoretical value of the MTF drops to zero at a spatial frequency of 4 μm^{-1}. Therefore the nominal limiting-resolution is estimated to

be 0.25 μm (0.125 μm line and 0.125 μm space).

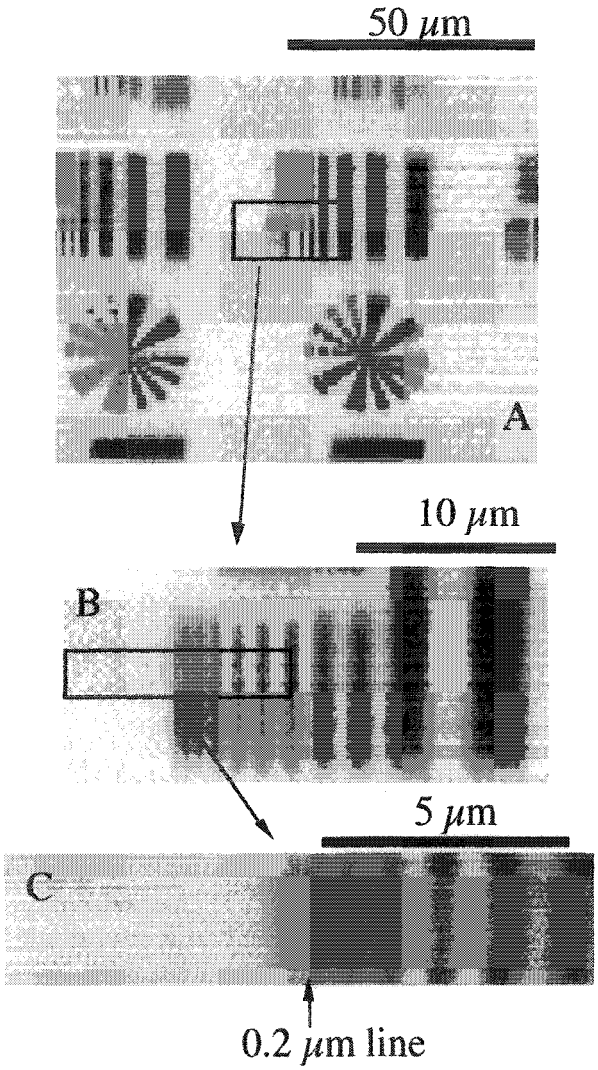

(a) Measured Image

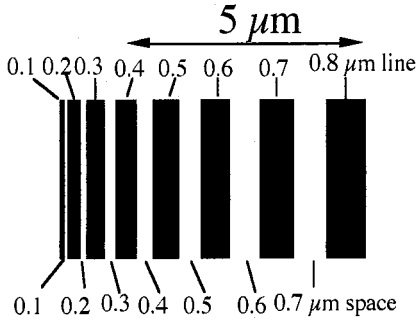

(b) Schematic Drawing of Resolution Test Pattern

Fig. 8. Fig. 4. Scanning microscopic images of test patterns. (a) Measured images. X-ray energy is 8 eV. Two-dimensional images are acquired by raster-scanning the sample. Image A: 100 x 80 pixels, pixel size: 1 μm x 1 μm, dwell time: 0.5 s/pixel. Image B: 100 x 45 pixels, 0.25 μm/pixel, dwell time: 0.5 s. Image C: 200 x 40 pixels, 0.0625 μm/pixel, dwell time: 0.5 s/pixel. (b)

Schematic drawing of the test pattern.

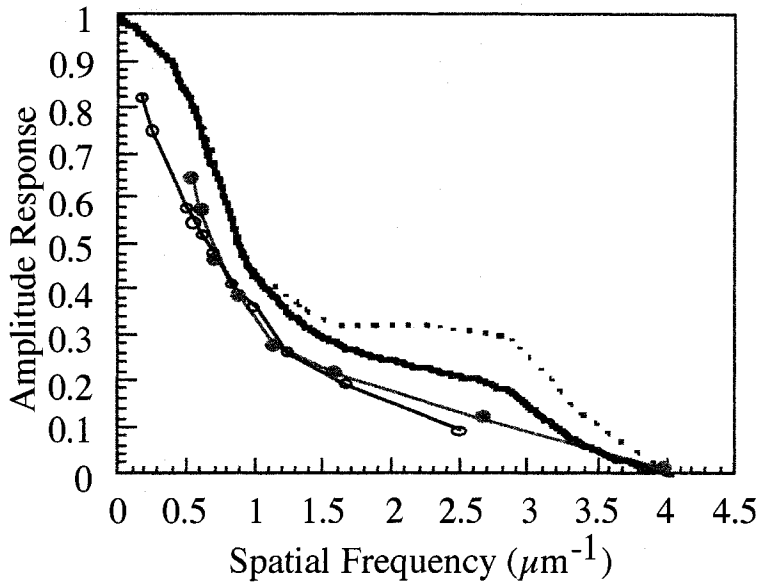

Fig. 9. Modulation transfer function. Dashed line: theoretical calculation for parallel beam illumination. Solid line: theoretical calculation assuming geometrical spot size of 0.18 μm. Closed circles are measured amplitude response derived from knife-edge scan profile. Open circle: MTF derived from measured images of scanning microscopy.

4. CONCLUSIONS

X-ray microbeam with the Fresnel zone plate optics has been tested at an X-ray energy region from 6 to 10 keV. By using fully coherent illumination, the focused beam size near to the diffraction-limited resolution has been achieved. The measured spot size defined by the full-width at half-maximum is 0.3 μm using the Fresnel zone plate of 0.25 μm outermost zone width. In the scanning microscopy experiment, spatial resolution better than 0.4 μm has been confirmed. These data suggest that the focused beam is almost coherent, and can be applied to Gabor type X-ray holography or X-ray speckle experiment.

REFERENCES

1) Y. Suzuki and F. Uchida: Rev. Sci. Instrum. **63** (1992) 578.
2) S. Aoki, A. Takeuchi, K. Sakurai, H. Kameno, D. Saito. H. Takano, K. Yamamoto, N. Watanabe, M. Ando, Y. Yoshidomi, K. Shinada and T. Kato: J. Phys. IV (France) **7** (1997) C2-329.
3) J. H. Underwood, A. C. Thompson, Y. Wu and R. D. Giauque: Nucl. Instrum. and Methods **A 266** (1988) 296.
4) J. H. Underwood, A. C. Thompson, J. B. Kortright, K. C. Chapman and D. Lunt: Rev. Sci. Instrum. **67** (1996) 3359
5) D. H. Bilderback, S. A. Hoffman and D. J. Thiel: Science **263** (1994) 201.
6) A. Erko, Y. Agafonov, L. A. Panchenko, A. Yakshin, P. Chevallier, O. Dhez and F. Legrand: Opt. Commun. **106** (1994) 146.
7) A. Snigirev, I. Snigireva, P. Engström, S. Lequien, A. Suvorov, Ya. Hartman, P. Chevallier, M. Idir, F. Legrand, G. Soullie and S. Engrand: Rev. Sci. Instrum. **66** (1995) 1461.
8) A. Snigirev: Rev. Sci. Instrum. **66** (1995) 2053.
9) Y. Suzuki, N. Kamijo, S. Tamura, K. Handa, A. Takeuchi, S. Yamamoto, H. Sugiyama, K. Ohsumi and M. Ando: J. Synchrotron Radiat. **4** (1997) 60.
10) Y. Suzuki, M. Awaji, Y. Kohmura, A. Takeuchi, N. Kamijo, S. Tamura and K. Handa: X-ray Microscopy, Proc. Sixth Int. Conf. ed. by W. Meyer-Ilse, T. Warwick and D. Attwood (American Institute of Physics, New York, 2000) p. 535.
11) W. Yun, B. Lai, Z. Cai, J. Maser, D. Legnini, E. Gluskin, Z. Chen, A. A. Krasnoperova, Y. Vladimirsky, F. Cerrina,

E. Di. Fabrizio, and M. Gentili, Rev. Sci. Instrum. **70** (1999) 2238.
12) Y. Kagoshima, K. Takai, T. Ibuki, K. Yokoyama, S. Takeda, M. Urakawa, Y. Tsusaka and J. Matsui: X-ray Microscopy, Proc. Sixth Int. Conf. ed. by W. Meyer-Ilse, T. Warwick and D. Attwood (American Institute of Physics, New York, 2000) p. 668
13) Y. Kohmura, M. Awaji, Y. Suzuki and T. Ishikawa: Proc. SPIE **3449** (1998) 185.
14) Y. Kohmura, M. Awaji, Y. Suzuki, T. Ishikawa, Y. I. Dudchik, N. N. Kolchevsky and F. F. Komarov: Rev. Sci. Instrum. **70** (1999) 4164.
15) B. Lengeler, C. G. Schroer, M. Richwin, J. Tuemmler, M. Drakopoulos, A. Snigirev and I. I. Snigireva: Appl. Phys. Lett. **74** (1999) 3924.
16) Y. Suzuki, A. Takeuchi, H. Takano, T. Ohigashi and H. Takenaka, Jpn. J. Appl. Phys. 40 (2001) 1508.
17) A. Ozawa, T. Tamamura, T. Ishii, H. Yoshihara and T. Kagoshima: Microelectron. Eng. **35** (1997) 525.
18) H. Kitamura: J. Synchrotron Radiat. **5** (1998) 184.
19) M. Born and E. Wolf: *Principles of Optics* (Pergamon, New York, 1980) 6th ed., p. 416.
20) B. L. Henke, E. M. Gullikson, and J. C. Davis, Atomic Data and Nuclear Data Tables 54 (1993) 181. The index of refraction used for the calculation is from the web site: www-cxro.bnl.gov/optical constant/